

## OPEN ACCESS

## EDITED BY

Khan M. G. Mostofa,  
Tianjin University, China

## REVIEWED BY

Zhaokai Xu,  
Institute of Oceanology (CAS), China  
Pier Christian van der Merwe,  
University of Tasmania, Australia

## \*CORRESPONDENCE

Jun Zhao

✉ jzhao@sio.org.cn

## SPECIALTY SECTION

This article was submitted to  
Marine Biogeochemistry,  
a section of the journal  
Frontiers in Marine Science

RECEIVED 11 January 2023

ACCEPTED 20 March 2023

PUBLISHED 29 March 2023

## CITATION

Huang W, Guo X, Zhao J, Li D, Hu J,  
Zhang H, Zhang C, Han Z, Sun W, Sun Y  
and Pan J (2023) Low content of highly  
reactive iron in sediments from Prydz Bay  
and the adjacent Southern Ocean:  
Controlling factors and implications for  
sedimentary organic carbon preservation.  
*Front. Mar. Sci.* 10:1142061.  
doi: 10.3389/fmars.2023.1142061

## COPYRIGHT

© 2023 Huang, Guo, Zhao, Li, Hu, Zhang,  
Zhang, Han, Sun, Sun and Pan. This is an  
open-access article distributed under the  
terms of the [Creative Commons Attribution  
License \(CC BY\)](https://creativecommons.org/licenses/by/4.0/). The use, distribution or  
reproduction in other forums is permitted,  
provided the original author(s) and the  
copyright owner(s) are credited and that  
the original publication in this journal is  
cited, in accordance with accepted  
academic practice. No use, distribution or  
reproduction is permitted which does not  
comply with these terms.

# Low content of highly reactive iron in sediments from Prydz Bay and the adjacent Southern Ocean: Controlling factors and implications for sedimentary organic carbon preservation

Wenhao Huang<sup>1,2</sup>, Xiaoze Guo<sup>1,2,3</sup>, Jun Zhao<sup>1,2\*</sup>, Dong Li<sup>1,2</sup>,  
Ji Hu<sup>1,2</sup>, Haifeng Zhang<sup>1,2</sup>, Cai Zhang<sup>1,2</sup>, Zhengbing Han<sup>2</sup>,  
Weiping Sun<sup>2</sup>, Yongge Sun<sup>3</sup> and Jianming Pan<sup>1,2</sup>

<sup>1</sup>Key Laboratory of Marine Ecosystem Dynamics, Ministry of Natural Resources, Hangzhou, China,

<sup>2</sup>Second Institute of Oceanography, Ministry of Natural Resources, Hangzhou, China, <sup>3</sup>Institute of Environmental and Biogeochemistry (eBig), School of Earth Sciences, Zhejiang University, Hangzhou, China

Examining iron (Fe) speciation in marine sediments is critical to understand Fe and carbon biogeochemical cycling in polar regions. In this study, we investigated the speciation of Fe in sediments from Prydz Bay and the adjacent Southern Ocean, and examined the factors controlling Fe speciation and its relationship with total organic carbon (TOC). Our results reveal that unreactive silicate Fe ( $Fe_U$ ) is the dominant pool of total Fe ( $Fe_T$ ), followed by poorly reactive sheet silicate Fe ( $Fe_{PRS}$ ), reducible crystalline Fe oxides ( $Fe_{ox2}$ ), easily reducible amorphous/poorly crystalline Fe oxides ( $Fe_{ox1}$ ), and magnetite ( $Fe_{mag}$ ), with carbonate-associated ferrous Fe ( $Fe_{carb}$ ) being the smallest pool. The highly reactive Fe ( $Fe_{HR}$ )/ $Fe_T$  ratios ( $0.13 \pm 0.06$ ) in our study area are among the lowest end-member globally, primarily due to weak bedrock weathering and slow glacier melting. The  $Fe_{ox1}/Fe_T$  ratios are similar to those in continental shelf and marginal seas containing highly weathered materials, while the  $Fe_{ox2}/Fe_T$  ratios are significantly lower. This result implicates that low temperature inhibits the aging of iceberg melting-sourced  $Fe_{ox1}$  potentially, and accordingly the regulation of weathering on the  $Fe_{HR}/Fe_T$  ratio is mainly reflected in  $Fe_{ox2}/Fe_T$  ratio. There are no significant correlations between TOC and  $Fe_{HR}$ ,  $Fe_{carb}$ ,  $Fe_{ox1}$  or  $Fe_{ox2}$  in the research region. Four distinct patterns of TOC/ $Fe_{HR}$  ratio can be discerned by summarizing the global data set: (a) high TOC/ $Fe_{HR}$  ratios ( $> 2.5$ ) are likely the result of high marine primary productivity and low chemically weathered source materials; (b) low TOC/ $Fe_{HR}$  ratios ( $< 0.6$ ) are caused by high rates of  $Fe_{HR}$  inputs and OC remineralization; (c) mid-range TOC/ $Fe_{HR}$  ratios ( $0.6 - 2.5$ ) typical of most river particulates and marginal sea sediments indicate the same  $Fe_{HR}$  and OC sources and/or interactions between each other; (d) both low TOC and  $Fe_{HR}$  content is the result of low marine primary productivity and weak chemical weathering. Our findings provide new insights into the relationship between  $Fe_{HR}$  and TOC in polar sediments.

## KEYWORDS

Fe speciation, highly reactive Fe, Southern Ocean, marine sediment, organic carbon

## 1 Introduction

The role of iron (Fe) speciation, rather than its total amount, is critical in Fe biogeochemical processes such as activity, migration, and bioavailability in marine sediments (Tagliabue et al., 2017). Due to its diverse mineralogy, crystallography, morphology, and chemical composition, Fe exhibits significant oxidation-reduction and adsorption reactivities (Kostka and Iii, 1994; Thamdrup, 2000). The sequential separation of different Fe species from the reaction phase is the foundation of Fe biogeochemistry (Poulton and Raiswell, 2005). Marine sediments serve as both a crucial Fe sink and source (Wadley et al., 2014; Homoky et al., 2016). The characteristics of Fe speciation in sediments are influenced by multiple factors, including the mixing of source materials with varying intensities of chemical weathering, bedrock type, redox conditions, pH values, chemical properties of organic matter, and diagenesis (Canfield, 1989; Poulton and Raiswell, 2005; Konhauser et al., 2011; Wehrmann et al., 2014; Thomasarrigo et al., 2019; Wei et al., 2021; Pasquier et al., 2022). Furthermore, highly reactive Fe ( $Fe_{HR}$ , operationally defined as Fe (oxyhydr)oxides and carbonates that readily react with sulfide to form sulfide minerals and eventually pyrite [Canfield, 1989]) in sediments has a significant impact on the biogeochemical cycling and fate of carbon (C) and other trace elements (Tagliabue et al., 2017). Therefore, the analysis of Fe speciation in sediments and the identification of controlling factors are crucial in studying Fe and C biogeochemical cycles.

Early studies demonstrated that Antarctic glacial sediments, which contain poorly chemically weathered material, exhibit significantly lower  $Fe_{HR}$  content and  $Fe_{HR}/total\ Fe\ (Fe_T)$  ratios compared to terrestrial riverine particulates (Poulton and Raiswell, 2002; Raiswell et al., 2006). Recent studies on polar regions have revealed that glacial runoff meltwater contributes additional  $Fe_{HR}$  to coastal Antarctic waters (Bhatia et al., 2013; Hawkings et al., 2014; Wehrmann et al., 2014; Lyons et al., 2015; Dinniman et al., 2020), presenting a promising opportunity to enhance primary productivity in the Southern Ocean and accelerate carbon dioxide consumption from the atmosphere in this region (Blain et al., 2007). Correspondingly, the  $Fe_{HR}$  content and  $Fe_{HR}/Fe_T$  ratio in Antarctic marine sediments may rise (Henkel et al., 2018). Given the increasing melting rate of Antarctic glaciers in recent decades (Shepherd et al., 2018), these impacts may become more significant. However, limited data on Fe species in Antarctic sediments pose challenges in assessing the impact of glacial melting on the biogeochemical cycles of Fe and C in polar regions under the context of global warming.

The natural process of “Fe fertilization”, which involves the transport of more  $Fe_{HR}$  to the ocean due to increased glacial melting, not only enhances the transport of organic carbon (OC)

to the deep sea (Pollard et al., 2009), but also has the potential to promote sedimentary OC burial. OC- $Fe_{HR}$  complexes formed by the combination of  $Fe_{HR}$  and OC exhibit long-term preservation potential (Lalonde et al., 2012; Faust et al., 2021), and their formation is therefore significant for improving the burial efficiency of marine sedimentary OC and mitigating global warming (Salvadó et al., 2015). However, the proportion of OC in OC- $Fe_{HR}$  complexes to total OC (TOC) ( $f_{OC-Fe}$ ) in global marine surface sediments varies widely (0.5% – 80%) (Lalonde et al., 2012; Longman et al., 2021; Longman et al., 2022). Fe speciation and  $Fe_{HR}$  content in different sedimentary environments are significantly differ, which may be a crucial factor influencing the degree of OC- $Fe_{HR}$  complexing (Ma et al., 2018; Faust et al., 2021). Therefore, investigating the species composition of  $Fe_{HR}$  in Antarctic marine sediments and its potential relationship with OC preservation is of great significance for comprehending the OC- $Fe_{HR}$  coupling mechanism and evaluating the response of the Antarctic C cycle to climate change.

Prydz Bay is the largest bay in the Indian Ocean sector of Antarctica. Its seaward perimeter is delineated by two shallower water depth banks, namely Fram Bank to the northwest and Four Ladies Bank to the northeast. The continental shelf region in Prydz Bay is comparable to that of the Weddell Sea and the Ross Sea, which are the two major Antarctic coastal seas and have the most productive coastal polynyas (Arrigo et al., 2015). However, Prydz Bay has fewer ice-free zones (Campbell et al., 1993) and less ice shelf melting (Shepherd et al., 2018; The IMBIE team, 2018), leading to weak chemical weathering and low  $Fe_{HR}$  inputs. The accumulation of marine materials in the surface sediments of Prydz Bay is primarily driven by primary production, as indicated by the distribution of chlorophyll a in surface waters and sedimentary TOC and total nitrogen (TN) (Vaz and Lennon, 1996; Liu et al., 2014). Therefore, Prydz Bay and the adjacent Southern Ocean provide an ideal area for studying Fe speciation and its relationship with OC, given the specific geographical environment and material source conditions.

In this study, we conducted the sequential extraction of Fe species and measured TOC,  $Fe_T$ , grain size and specific surface area (SSA) in 20 surface sediments from Prydz Bay and the adjacent Southern Ocean. The aim was to characterize the distribution of Fe species, particularly  $Fe_{HR}$ , and speculate on its controlling factors. Additionally, we preliminarily discussed the relationship between TOC and Fe speciation in the research region and the implications from a global perspective.

## 2 Materials and methods

### 2.1 Sampling procedure

During the 24<sup>th</sup> to 29<sup>th</sup> Chinese National Antarctic Research Expeditions (CHINARE-24 to -29, 2007 – 2013), a total of 20 surface sediment samples were collected from Prydz Bay and the adjacent Southern Ocean (Figure 1; Table 1). The box sampler was used to collect the sediment samples, and the topmost 0 – 1 cm layer was considered as the surface sample. The samples were

**Abbreviations:**  $Fe_{carb}$ , carbonate associated ferrous Fe;  $Fe_{ox1}$ , easily reducible amorphous/poorly crystalline Fe oxides (ferrihydrite, lepidocrocite);  $Fe_{ox2}$ , reducible crystalline Fe oxides (goethite, akaganéite, hematite);  $Fe_{mag}$ , magnetite;  $Fe_{PRS}$ , poorly reactive sheet silicate Fe;  $Fe_T$ , Total Fe;  $Fe_{HR}$ , Highly reactive Fe ( $Fe_{carb} + Fe_{ox1} + Fe_{ox2} + Fe_{mag}$ );  $Fe_U$ , Unreactive silicate Fe ( $Fe_T - Fe_{HR} - Fe_{PRS}$ ); SSA, Specific surface area; TOC, Total organic carbon;  $f_{OC-Fe}$ , Proportion of OC in OC- $Fe_{HR}$  complexes to TOC.

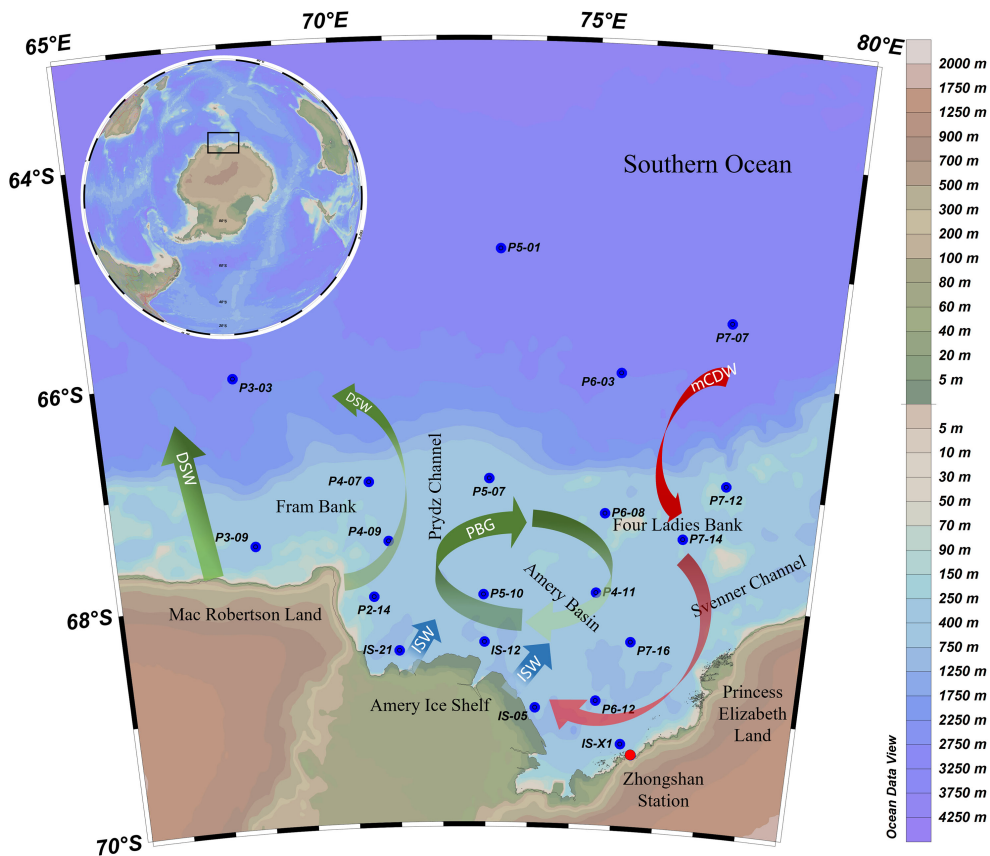


**FIGURE 1** Surface sediment sampling stations in Prydz Bay and the adjacent Southern Ocean during the 24<sup>th</sup> to 29<sup>th</sup> Chinese National Antarctic Research Expeditions (CHINARE-24 to -29). The circumfluence map is modified after Williams et al. (2016). PBG, Prydz Bay Gyre; mCDW, modified Circumpolar Deep Water; DSW, Dense Shelf Water; ISW, Ice Shelf Water.

**TABLE 1** Sampling information, sand, clay, silt and categories of surface sediment from Prydz Bay and the adjacent Southern Ocean.

Station	Longitude (°E)	Latitude (°S)	Water Depth (m)	Cruise	Silt (%)	Sand (%)	Clay (%)	Category
P4-09	70.87	67.52	285	CHINARE-29	22.1	72.7	5.12	Coarse
P4-07	70.49	66.99	293	CHINARE-29	25.5	68.7	5.75	
P7-12	78.00	66.94	218	CHINARE-29	41.3	51.5	7.15	Medium
IS-05	74.11	68.99	707	CHINARE-24	39.5	50.6	9.84	
IS-21	71.05	68.49	777	CHINARE-27	51.5	38.6	9.88	
P5-07	73.02	66.97	510	CHINARE-29	48.2	40.0	11.8	Fine
P7-14	77.18	67.44	312	CHINARE-29	45.9	37.1	17.1	
P5-10	72.92	68.00	642	CHINARE-29	62.3	21.1	16.5	
P7-16	76.20	68.38	559	CHINARE-29	65.1	17.5	17.5	
P3-09	68.01	67.51	251	CHINARE-29	72.8	15.3	11.9	Fine
IS-12	72.95	68.42	748	CHINARE-27	72.4	14.1	13.5	
P2-14	70.52	68.01	496	CHINARE-25	69.0	18.1	12.9	
P4-11	75.38	67.96	491	CHINARE-24	81.9	2.75	15.4	

(Continued)

TABLE 1 Continued

Station	Longitude (°E)	Latitude (°S)	Water Depth (m)	Cruise	Silt (%)	Sand (%)	Clay (%)	Category
IS-X1	76.11	69.28	/	CHINARE-27	79.5	3.69	16.8	Ultra-fine
P6-12	75.49	68.91	700	CHINARE-29	75.1	8.14	16.7	
P6-08	75.49	67.25	386	CHINARE-29	66.8	8.29	24.9	
P6-03	75.68	65.99	2920	CHINARE-29	60.7	12.9	26.4	
P7-07	77.82	65.48	3250	CHINARE-29	61.5	11.7	26.9	
P5-01	73.21	64.90	3421	CHINARE-29	55.5	16.8	27.7	
P3-03	67.81	66.00	2689	CHINARE-29	51.0	9.03	40.0	

immediately frozen at  $-20^{\circ}\text{C}$  and transported to the laboratory where they were stored at the same temperature until analysis.

## 2.2 Grain size and specific surface area analysis

The sediment grain size was analyzed using a laser particle size analyzer (Malvern Mastersizer 3000, UK) with an analysis range of  $0.01 - 3500 \mu\text{m}$  and a precision better than 1%. Approximately 1 g of wet sediment was placed into pure water and mixed well with ultrasonication. The bulk sediment samples were then separated into 3 standard size fractions: sand ( $> 63 \mu\text{m}$ ), silt ( $4 - 63 \mu\text{m}$ ), and clay ( $< 4 \mu\text{m}$ ). The freeze-dried sediments were heated in a muffle oven at  $350^{\circ}\text{C}$  for 12 h to remove organic matter. The SSA of the sediments was measured by the static volumetric method using an automatic analyzer (Bessed 3H-2000 PS1, China) with an analysis range of  $> 0.005 \text{ m}^2/\text{g}$  and a precision better than 1%.

## 2.3 TOC analysis

The TOC content in the sediments was determined using an elemental analyzer–isotope ratio mass spectrometer (EA–IRMS) (Thermo Delta V advantage, US). The freeze-dried sediment samples were analyzed after removing carbonates by acid fumigation and oven drying at  $60^{\circ}\text{C}$  for 24 h (Harris et al., 2001). The precision of the reference material (Acetanilide) was  $\pm 0.23\%$  ( $n = 5$ ). One sample was selected to run as replicates in parallel (P7-16), and the relative standard deviation (RSD) of TOC measurements was  $< 16\%$  ( $n = 2$ , Table S2).

## 2.4 Total Fe and Al determination

The  $\text{Fe}_T$  and Al content were analyzed using an inductively coupled plasma–atomic emission spectrometer (ICP–AES) (Thermo Fisher IRIS Intrepid II XSP, US). The freeze-dried sediment samples were placed in a polytetrafluoroethylene inner tank, which was immersed in nitric acid and leached with deionized water. The samples were then digested with mixed  $\text{HF-HClO}_4\text{-HNO}_3$  acids (guaranteed reagent) in a microwave digestion

instrument. The acid was expelled, and the volume was calibrated by adding Rhodium. The  $\text{Fe}_T$  and Al content in the digestion fluid were determined by subtracting blanks. Reference materials (GBW07314 [offshore marine sediments, The State Bureau of Quality and Technical Supervision of China], GBW07103 [granite rock composition analysis reference materials, The State Bureau of Quality and Technical Supervision of China] and GSP-2 [granodiorite powdered reference materials, USGS]) were also digested using the same method for quality control. The recovery efficiencies of  $\text{Fe}_T$  and Al for the reference materials were 100.2% – 101.9% and 100.1% – 100.4%, respectively. Replicates were analyzed for two samples (P4-07, P7-07), and the RSDs were  $\leq 5.3\%$  ( $n = 2$ , Table S2).

## 2.5 Fe speciation

Fe species analyses, including carbonate associated ferrous Fe ( $\text{Fe}_{\text{carb}}$ ), easily reducible amorphous/poorly crystalline Fe oxides ( $\text{Fe}_{\text{ox1}}$ ), reducible crystalline Fe oxides ( $\text{Fe}_{\text{ox2}}$ ), magnetite ( $\text{Fe}_{\text{mag}}$ ), and poorly reactive sheet silicate Fe ( $\text{Fe}_{\text{PRS}}$ ), were conducted following the methods of Poulton and Canfield (2005) and März et al. (2012) as shown in Table S1. Briefly, the surface sediments were homogenized after freeze-drying, weighed accurately to 0.1 g, and then sequentially extracted by adding the respective reagents necessary for each Fe species to the centrifuge tube containing the sediments. The tubes were centrifuged at 4800 rpm for 10 min and the supernatants were transferred into PET bottles for Fe species analysis. The sediment residuals from the previous step were then washed twice with distilled water, which was added to the extracted supernatants. The Fe content in the supernatants was determined on a flame atomic absorption spectrophotometer (ZEE nit 700P, Germany). The RSDs for 10 samples were  $< 6.5\%$  for  $\text{Fe}_{\text{carb}}$ ,  $< 8.2\%$  for  $\text{Fe}_{\text{ox1}}$ ,  $< 4.9\%$  for  $\text{Fe}_{\text{ox2}}$ ,  $< 13\%$  for  $\text{Fe}_{\text{mag}}$  ( $n = 3$ ); and the RSDs for 2 samples was  $< 5.5\%$  for  $\text{Fe}_{\text{PRS}}$  ( $n = 2$ ) (Table S2). The sediments exhibited no observable indications of Fe sulfides (black mottles), leading to the assumption that pyrite-bound Fe was insignificant (März et al., 2012) and was not subject to analysis in this study. Here, we established  $\text{Fe}_{\text{HR}} = \text{Fe}_{\text{carb}} + \text{Fe}_{\text{ox1}} + \text{Fe}_{\text{ox2}} + \text{Fe}_{\text{mag}}$  as per Poulton and Canfield (2005). Consequently, the equation for unreactive silicate Fe ( $\text{Fe}_U$ ) was:  $\text{Fe}_U = \text{Fe}_T - (\text{Fe}_{\text{HR}} + \text{Fe}_{\text{PRS}})$ .

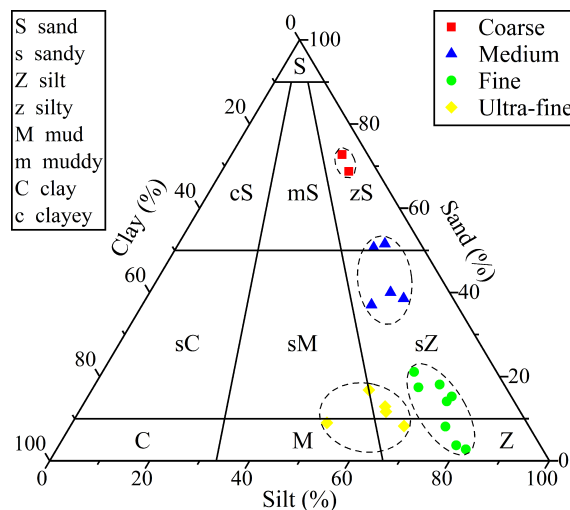


**FIGURE 2**  
Classification of surface sediments in Prydz Bay and the adjacent Southern Ocean. Samples are classified into 4 categories based on a cluster analysis: “Coarse” (red squares), “Medium” (blue triangles), “Fine” (green dots) and “Ultra-fine” (yellow diamonds).

## 2.6 Statistical analyses

To establish relationships between the measured parameters, a Pearson correlation analysis and a two-tailed test of significance were conducted using the statistical software SPSS (Version 25). Additionally, a cluster analysis was performed using the same software. One-way analysis of variance with a 95% confidence interval ( $p < 0.05$ ) was used to identify statistically significant differences.

## 3 Results

### 3.1 Grain size and grouping

The sediment composition in the study area is analyzed in terms of the content of clay (5.12% – 40.0%), sand (2.75% – 72.7%), and silt (22.1% – 81.9%). Silt is found to be the dominant component,

accounting for an average of 57.4% of the sediment volume (Table S3). Sandy silt is identified as the main sediment type in the study area (Figure 2) according to the sediment classification method of Folk (1980). Cluster analysis of grain size results in the division of sediment samples into 4 categories: “Coarse”, “Medium”, “Fine” and “Ultra-fine”, as shown in Figure 2. The “Coarse” category includes 2 stations from Fram Bank, the “Medium” category includes 5 stations from the Amery Ice Shelf front, Four Ladies Bank and Prydz Channel, the “Fine” category includes 8 stations from the Cape Darnley polynya and Amery Basin, and the “Ultra-fine” category includes 5 stations from the deep Southern Ocean and Four Ladies Bank (Table 1).

### 3.2 SSA, TOC and OC loading

The SSA of the sediment samples ranges from 1.78 to 41.2 m<sup>2</sup>/g. The highest SSA is found in the “Ultra-fine” sediment category

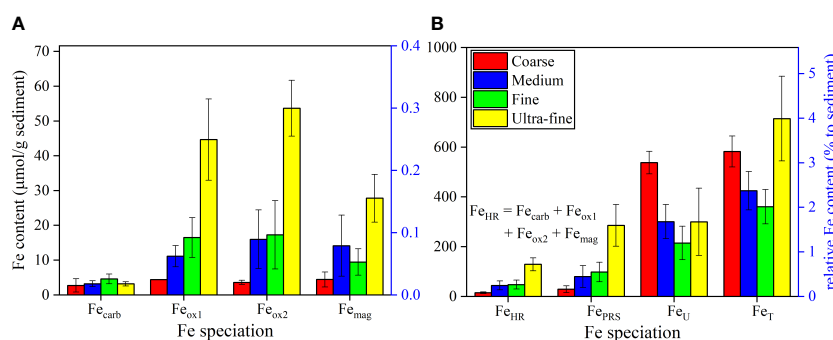


**FIGURE 3**  
The average content of (A)  $Fe_{carb}$ ,  $Fe_{ox1}$ ,  $Fe_{ox2}$ ,  $Fe_{mag}$  and (B)  $Fe_{HR}$ ,  $Fe_{PRS}$ ,  $Fe_U$ ,  $Fe_T$  in “Coarse”, “Medium”, “Fine” and “Ultra-fine” categories of sediments from Prydz Bay and the adjacent Southern Ocean. Note:  $Fe_{HR} = Fe_{carb} + Fe_{ox1} + Fe_{ox2} + Fe_{mag}$ .

( $33.9 \pm 8.13 \text{ m}^2/\text{g}$ ), followed by “Fine” ( $17.7 \pm 4.86 \text{ m}^2/\text{g}$ ) and “Medium” ( $8.57 \pm 4.06 \text{ m}^2/\text{g}$ ) sediments. The “Coarse” sediment category has the lowest SSA ( $1.87 \pm 0.128 \text{ m}^2/\text{g}$ ) (Table S3).

The TOC content ranges from 0.13% to 1.65%, similar to values (0.14% – 1.20%) in Liu et al. (2014). The “Fine” sediment category has significantly ( $p < 0.005$ ) higher TOC content ( $1.02\% \pm 0.35\%$ ) than the other 3 categories ( $0.19\% \pm 0.02\%$ ,  $0.32\% \pm 0.28\%$ ,  $0.34\% \pm 0.19\%$  for “Coarse”, “Medium” and “Ultra-fine”, respectively) (Table S3).

The OC loading (i.e., the TOC/SSA ratio) ranges from 0.04 to  $1.29 \text{ mg}/\text{m}^2$ . The “Coarse” sediment category has the highest OC loading ( $0.99 \pm 0.18 \text{ mg}/\text{m}^2$ ), followed by “Fine” ( $0.62 \pm 0.33 \text{ mg}/\text{m}^2$ ), “Medium” ( $0.38 \pm 0.21 \text{ mg}/\text{m}^2$ ), and “Ultra-fine” ( $0.12 \pm 0.11 \text{ mg}/\text{m}^2$ ) sediments (Table S3).

### 3.3 Total Fe and Fe speciation

The  $\text{Fe}_T$  content ranges from 1.22% to 5.19% ( $2.72\% \pm 0.993\%$ ), and is significantly ( $p < 0.01$ ) higher in the “Ultra-fine” category sediments ( $3.99\% \pm 0.950\%$ ) than “Fine” ( $2.01\% \pm 0.387\%$ ) and “Medium” ( $2.37\% \pm 0.430\%$ ) sediments, with the middle value in “Coarse” category ( $3.25\% \pm 0.348\%$ ) (Table S3).

The characteristics of Fe speciation are reported in Table S3. A comparison of the average yields of various Fe pools and their ratios to  $\text{Fe}_T$  in the 4 grain size categories are shown in Figure 3.  $\text{Fe}_U$  is the largest Fe pool ( $290 \pm 125 \text{ } \mu\text{mol}/\text{g}$ ), followed by  $\text{Fe}_{\text{PRS}}$  ( $134 \pm 105 \text{ } \mu\text{mol}/\text{g}$ ) and  $\text{Fe}_{\text{HR}}$  ( $64.0 \pm 43.7 \text{ } \mu\text{mol}/\text{g}$ ) (Figure 3B). Within  $\text{Fe}_{\text{HR}}$ , the content of  $\text{Fe}_{\text{ox}2}$  ( $24.7 \pm 19.4 \text{ } \mu\text{mol}/\text{g}$ ) and  $\text{Fe}_{\text{ox}1}$  ( $21.0 \pm 15.9 \text{ } \mu\text{mol}/\text{g}$ ) is significantly ( $p < 0.001$ ) higher than  $\text{Fe}_{\text{carb}}$  ( $3.70 \pm 1.31 \text{ } \mu\text{mol}/\text{g}$ ), with  $\text{Fe}_{\text{mag}}$  in the mid-range of these values ( $14.7 \pm 9.99 \text{ } \mu\text{mol}/\text{g}$ ) (Figure 3A).

Regarding different grain size categories,  $\text{Fe}_{\text{ox}1}$ ,  $\text{Fe}_{\text{ox}2}$ ,  $\text{Fe}_{\text{mag}}$ ,  $\text{Fe}_{\text{HR}}$  and  $\text{Fe}_{\text{PRS}}$  content is all significantly ( $p < 0.01$ ) higher in “Ultra-fine” sediments ( $44.6 \pm 11.7$ ,  $53.7 \pm 8.02$ ,  $27.8 \pm 6.87$ ,  $129 \pm 26.0$ ,  $285 \pm 83.6 \text{ } \mu\text{mol}/\text{g}$ , respectively) than “Coarse” ( $4.37 \pm 0.0778$ ,  $3.59 \pm 0.601$ ,  $4.42 \pm 2.16$ ,  $15.1 \pm 3.37$ ,  $29.5 \pm 13.5 \text{ } \mu\text{mol}/\text{g}$ , respectively), “Medium” ( $11.1 \pm 3.04$ ,  $16.0 \pm 8.44$ ,  $14.1 \pm 8.82$ ,  $44.4 \pm 17.7$ ,  $80.0 \pm 43.9 \text{ } \mu\text{mol}/\text{g}$ , respectively) and “Fine” ( $16.5 \pm 5.73$ ,  $17.2 \pm 9.82$ ,  $9.43 \pm 3.79$ ,  $47.7 \pm 17.9$ ,  $98.0 \pm 39.1 \text{ } \mu\text{mol}/\text{g}$ , respectively) categories.  $\text{Fe}_U$  is significantly ( $p < 0.01$ ) higher in “Coarse” sediments ( $538 \pm 45.5 \text{ } \mu\text{mol}/\text{g}$ ) than in “Medium” ( $300 \pm 68.6 \text{ } \mu\text{mol}/\text{g}$ ), “Fine” ( $215 \pm 67.4 \text{ } \mu\text{mol}/\text{g}$ ) and “Ultra-fine” ( $300 \pm 135 \text{ } \mu\text{mol}/\text{g}$ ) sediments, while there is no significant difference ( $p > 0.05$ ) in  $\text{Fe}_{\text{carb}}$  ( $2.72 \pm 1.90$ ,  $3.20 \pm 0.830$ ,  $4.59 \pm 1.41$  and  $3.16 \pm 0.605 \text{ } \mu\text{mol}/\text{g}$  for “Coarse”, “Medium”, “Fine” and “Ultra-fine” categories, respectively) (Figure 3).

## 4 Discussion

### 4.1 $\text{Fe}_{\text{HR}}$ characteristics and controlling factors

#### 4.1.1 Control of weak weathering and slow glacier melting on low $\text{Fe}_{\text{HR}}/\text{Fe}_T$ ratio

In the sediments from Prydz Bay and the adjacent Southern Ocean, there is a significant positive correlation between  $\text{Fe}_{\text{HR}}$  and  $\text{Fe}_T$ , as well as between  $\text{Fe}_{\text{HR}}$  and Al ( $R^2 = 0.55$ ,  $p < 0.001$ ;  $R^2 = 0.31$ ,  $p < 0.05$ ; Figure S1). This finding is consistent with the global riverine and glacial particulates, implying that  $\text{Fe}_{\text{HR}}$  are closely associated with Fe-bearing aluminosilicate minerals (Poulton and Raiswell, 2002; Poulton and Raiswell, 2005). The  $\text{Fe}_{\text{HR}}/\text{Fe}_T$  ratios in the research region ( $0.13 \pm 0.06$ ) are similar to those in Antarctic

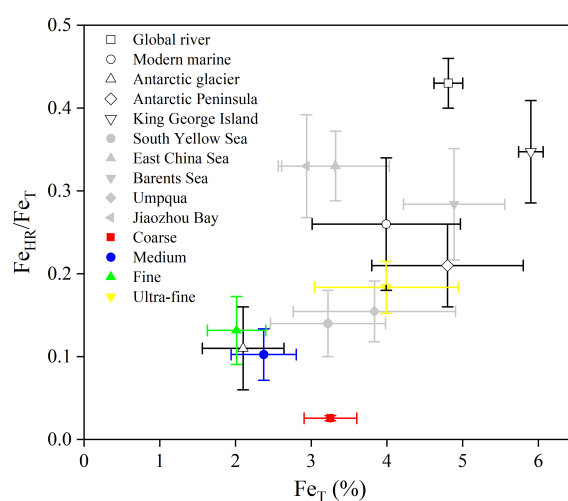


FIGURE 4

Comparison of  $\text{Fe}_{\text{HR}}/\text{Fe}_T$  and  $\text{Fe}_T$  in “Coarse”, “Medium”, “Fine” and “Ultra-fine” categories of sediments from Prydz Bay and the adjacent Southern Ocean with global riverine particulates and modern marine sediments, Antarctic glaciers (Raiswell and Canfield, 1998; Poulton and Raiswell, 2002), off the western Antarctic Peninsula (Burdige and Christensen, 2022), off King George Island (Henkel et al., 2018), South Yellow Sea (Ma et al., 2018), East China Sea (Zhu et al., 2012), Barents Sea (Faust et al., 2021), Umpqua (Roy et al., 2013) and the Jiaozhou Bay (Zhu et al., 2015). Data are averages of surface sediments (0 – 2 cm) by recalculation of Henkel et al. (2018) and Burdige and Christensen (2022).

glacial particulates ( $0.11 \pm 0.05$ ), and lower than those in global river particulates ( $0.43 \pm 0.03$ ) and modern marine sediments ( $0.26 \pm 0.08$ ) (Figure 4) (Poulton and Raiswell, 2002). This result suggests that the sediments in our study area are mainly influenced by weak chemical weathering. Generally, during chemical weathering, the easily solubilized major elements (such as Na, K, Ca, etc.) in rock minerals are leached, while the insoluble elements, such as Al and Fe, are enriched. As a result, Fe forms insoluble mineral phases (mainly Fe oxides) that continuously adsorb on the surface of parent rock minerals (Martin and Meybeck, 1979; Canfield, 1997). Therefore, the degree of chemical weathering can determine the  $Fe_{HR}$  content as well as the  $Fe_{HR}/Fe_T$  ratio (Poulton and Raiswell, 2002; Wei et al., 2021).

River and glacier particulates are known to represent the high and low end-members of weathering intensity, respectively, and their mixing in varying proportions determines the  $Fe_{HR}/Fe_T$  ratio characteristics of sediments in different marine environments (Poulton and Raiswell, 2005). In the research region, the  $Fe_{HR}/Fe_T$  ratios belong to the lower end-member compared to other polar sediments (Figure 4). For example, in the Arctic Barents Sea, off the Antarctic Peninsula and King George Island, the  $Fe_{HR}/Fe_T$  ratios of surface sediments (shallower than 2 cm) are  $0.28 \pm 0.07$ ,  $0.21 \pm 0.05$  and  $0.35 \pm 0.06$ , respectively (Henkel et al., 2018; Faust et al., 2021; Burdige and Christensen, 2022), all significantly ( $p < 0.01$ ) higher than our result ( $0.13 \pm 0.06$ ) (Figure 4). This difference can be attributed to the differences in the glacier melting and the bedrock weathering. In our study region, the ice-free area is small and the glacier melting rate is slow (Campbell et al., 1993; The IMBIE team, 2018). However, in the Arctic Barents Sea, off the Antarctic Peninsula and King George Island, there are larger ice-free zones and higher glacier melting rates (Stammerjohn et al., 2008; Screen and

Simmonds, 2010; Rueckamp et al., 2011; The IMBIE team, 2018). Therefore, intense weathering process occurs: the runoff formed from ice melting continuously erodes the bedrock, producing soluble  $Fe^{2+}$  and secondary nanoparticulates, which are then oxidized and aged into Fe oxides, and transported to the marginal seas along with the runoff (Henkel et al., 2018). This situation is similar to those in rivers of middle and low latitudes, which can continuously transport Fe-containing particulates with high  $Fe_{HR}/Fe_T$  ratio. Besides, the  $Fe_{HR}/Fe_T$  ratios are significantly ( $p < 0.05$ ) higher off King George Island (Figure 4), probably due to the semi-enclosed bay topography, which is conducive to  $Fe_{HR}$  enrichment, similar to the Jiaozhou Bay and Bohai Sea (Zhu et al., 2015; Wang et al., 2019).

Our findings demonstrate that the  $Fe_{HR}/Fe_T$  ratios vary across the 4 grain size-based sediment categories in the study area. Specifically, the  $Fe_T$  content in “Coarse” sediments ( $3.25\% \pm 0.348\%$ ) is comparable to that of the Earth’s crust (3.5%) (Taylor, 1964), and the  $Fe_{HR}/Fe_T$  ratios are extremely low ( $0.03 \pm <0.005$ ), representing minimal weathering of the input material from the Antarctic continent. In “Medium” and “Fine” sediments, the  $Fe_T$  content ( $2.37\% \pm 0.430\%$  and  $2.01\% \pm 0.387\%$ , respectively) and  $Fe_{HR}/Fe_T$  ratios ( $0.10 \pm 0.03$  and  $0.13 \pm 0.04$ , respectively) are comparable to those of the Antarctic glacial particulates ( $2.10\% \pm 0.539\%$  and  $0.11 \pm 0.05$ ) (Poulton and Raiswell, 2002), indicating that sediments along the shelf of Prydz Bay primarily originate from the weak weathering Antarctic continent. While in “Ultra-fine” sediments, mainly from the deep Southern Ocean, the  $Fe_T$  content ( $3.99\% \pm 0.950\%$ ) is comparable to that of global deep sea sediments ( $4.29\% \pm 0.98\%$ ), and the  $Fe_{HR}/Fe_T$  ratios ( $0.18 \pm 0.03$ ) are slightly lower than those in global deep sea sediments ( $0.25 \pm 0.10$ ) (Poulton and Raiswell, 2002), indicating relatively enhanced weathering in this sediment category.

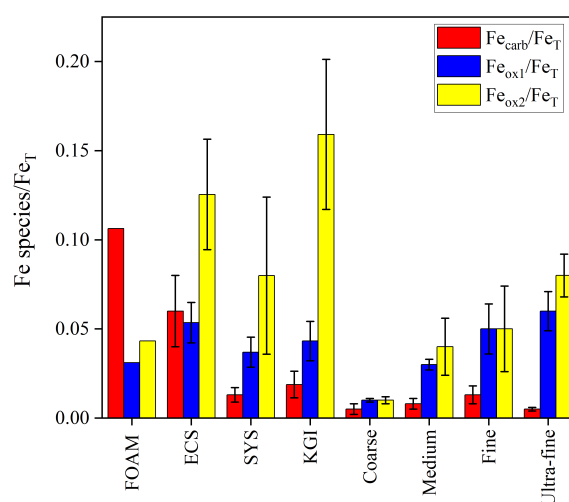


FIGURE 5

$Fe_{carb}/Fe_T$ ,  $Fe_{ox1}/Fe_T$  and  $Fe_{ox2}/Fe_T$  ratios in “Coarse”, “Medium”, “Fine” and “Ultra-fine” categories of sediments from Prydz Bay and the adjacent Southern Ocean, as well as in sediments from FOAM (friends of anoxic mud) (Canfield, 1989), the ECS (East China Sea) (Zhu et al., 2012), SYS (South Yellow Sea) (Ma et al., 2018) and KGI (King George Island) (Henkel et al., 2018). Data are averages of surface sediments (0 – 2 cm) by recalculation of Canfield (1989) and Henkel et al. (2018).

#### 4.1.2 Indications of the relative content of $\text{Fe}_{\text{carb}}$ , $\text{Fe}_{\text{ox1}}$ and $\text{Fe}_{\text{ox2}}$

The  $\text{Fe}_{\text{carb}}/\text{Fe}_{\text{T}}$  ratios of the 4 grain size-based sediment categories in our research region ( $0.005 \pm 0.003$ ,  $0.008 \pm 0.003$ ,  $0.013 \pm 0.005$  and  $0.005 \pm 0.001$  for “Coarse”, “Medium”, “Fine” and “Ultra-fine” categories, respectively) exhibit similarity ( $p > 0.05$ ) to values from oxygen-rich sedimentary environments (e.g.,  $0.013 \pm 0.004$  and  $0.019 \pm 0.007$  for the South Yellow Sea and off King George Island, respectively) (Henkel et al., 2018; Ma et al., 2018), but are significantly ( $p < 0.001$ ) lower than those from anoxic or hypoxic sedimentary environments (e.g.,  $0.11$  and  $0.06 \pm 0.02$  for FOAM and the East China Sea, respectively) (Canfield, 1989; Zhu et al., 2012) (Figure 5). Generally, in an Fe-rich and sulfide-free hypoxic or anoxic environment, intense microbially-mediated dissimilatory Fe reduction promotes the transformation of  $\text{Fe}_{\text{ox1}}$  and  $\text{Fe}_{\text{ox2}}$  to Fe(II) (Canfield, 1989; Mathew et al., 2022). Under neutral pH and oxidizing conditions, Fe(II) can rapidly oxidize to Fe(III) and hydrolyze to Fe (hydrogen)oxides (Konhauser et al., 2011; Ma et al., 2018). Therefore, our results indicate that the formation and accumulation of Fe(II) are restricted in oxygen-rich Antarctic marine environments (Meijers et al., 2010; Katsumata et al., 2015).

Interestingly, the  $\text{Fe}_{\text{ox2}}/\text{Fe}_{\text{T}}$  ratios of the 4 categories in our research region ( $0.01 \pm <0.005$ ,  $0.04 \pm 0.02$ ,  $0.05 \pm 0.02$  and  $0.08 \pm 0.01$  for “Coarse”, “Medium”, “Fine” and “Ultra-fine” categories, respectively) are significantly ( $p < 0.001$ ) lower than those in highly weathered marginal seas, such as the East China Sea and off King George Island ( $0.13 \pm 0.03$  and  $0.16 \pm 0.04$ ) (Zhu et al., 2012; Henkel et al., 2018). However, the  $\text{Fe}_{\text{ox1}}/\text{Fe}_{\text{T}}$  ratios ( $0.03 \pm <0.005$ ,  $0.05 \pm 0.01$  and  $0.06 \pm 0.01$  for “Medium”, “Fine” and “Ultra-fine” categories, respectively) are similar ( $p > 0.05$ ) to those from the East China Sea, South Yellow Sea, and off King George Island ( $0.05 \pm 0.01$ ,  $0.04 \pm 0.01$  and  $0.04 \pm 0.01$ ) (Zhu et al., 2012; Henkel et al., 2018; Ma et al., 2018) (Figure 5).

There are 3 potential explanations for the observed differences in patterns between  $\text{Fe}_{\text{ox1}}/\text{Fe}_{\text{T}}$  and  $\text{Fe}_{\text{ox2}}/\text{Fe}_{\text{T}}$ . Firstly, the transformation of  $\text{Fe}_{\text{ox1}}$  to  $\text{Fe}_{\text{ox2}}$  in the sediments of our study area is restricted. Generally, the initial Fe oxides in the redox cycle are highly reactive and amorphous: i.e.,  $\text{Fe}_{\text{ox1}}$ . Over time,  $\text{Fe}_{\text{ox1}}$  gradually transforms into more stable and crystalline Fe oxides: i.e.,  $\text{Fe}_{\text{ox2}}$  (Senn et al., 2017). However, the half-life of Fe oxides aging in low temperature environments ( $< 0^\circ\text{C}$ ) is 4 – 6 times longer than in mid-latitude areas ( $15^\circ\text{C} - 20^\circ\text{C}$ ) (Canfield et al., 1992; Raiswell and Canfield, 1998; Schwertmann et al., 2004). Considering the relatively new surface sediment ages in the continental shelf of Prydz Bay (Wu et al., 2017), the insufficient conversion time may be responsible for the low  $\text{Fe}_{\text{ox2}}/\text{Fe}_{\text{T}}$  ratios observed.

Secondly, there may be additional  $\text{Fe}_{\text{ox1}}$  sources in the study area. Icebergs are considered to be an important  $\text{Fe}_{\text{HR}}$  source to the Southern Ocean (Lin et al., 2011; Raiswell et al., 2016; Raiswell et al., 2018). The Fe in icebergs is often isolated by the ice, limiting Fe contact with water and organic matter and preventing Fe from further aging (Raiswell et al., 2016; Raiswell et al., 2018). Therefore, a high content of ferrihydrite exists in icebergs and may rapidly settle into sediments during melting by scavenging. However, due to a lack of systematic studies, it is still impossible to quantitatively

assess the importance of iceberg contributions to sedimentary Fe pools, especially  $\text{Fe}_{\text{ox1}}$ .

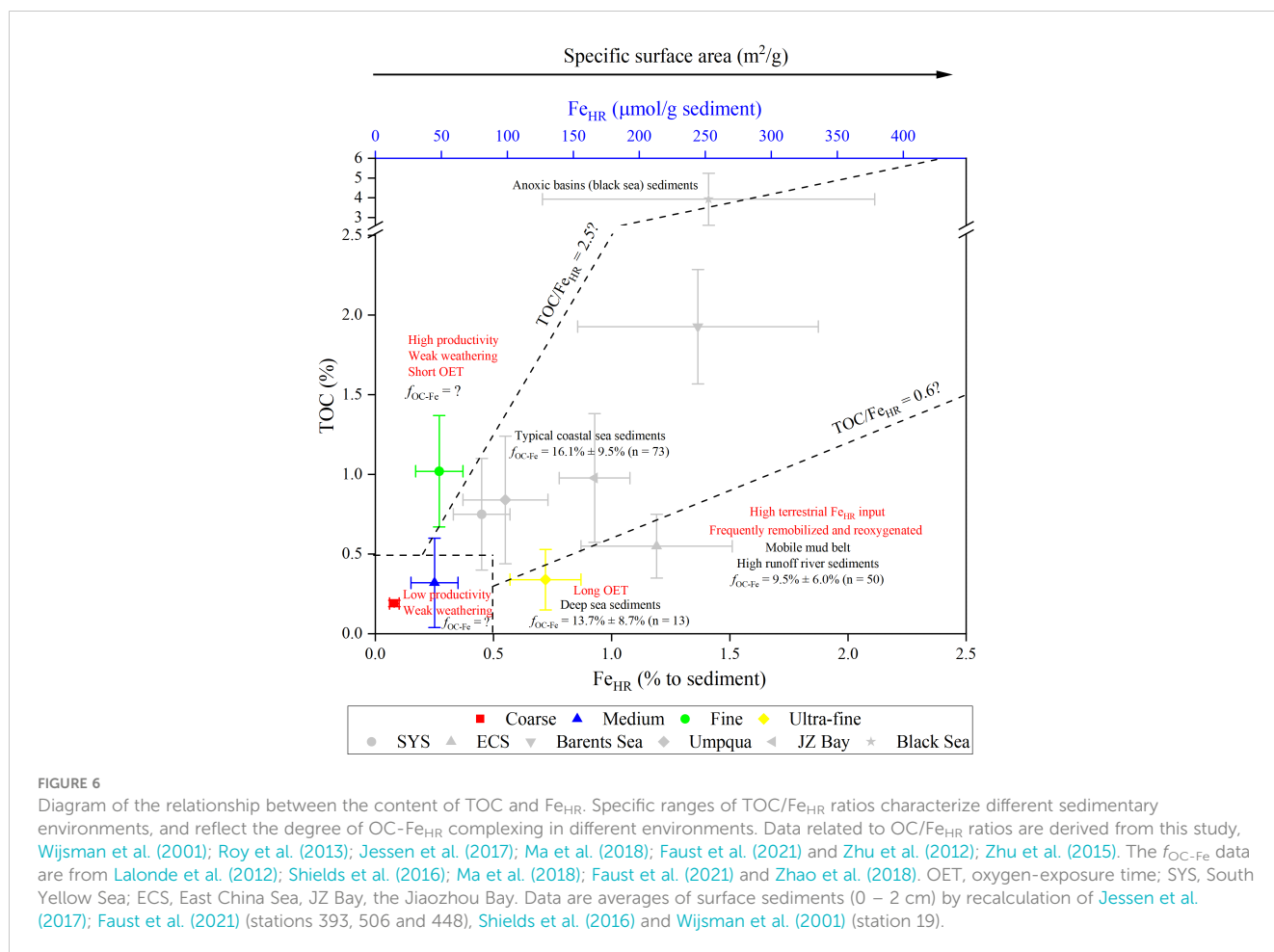
Finally, the dynamic equilibrium of the conversion between the transformation from  $\text{Fe}_{\text{ox1}}$  to  $\text{Fe}_{\text{ox2}}$  promoted by aging and the transformation from  $\text{Fe}_{\text{T}}$  to  $\text{Fe}_{\text{ox1}}$  promoted by chemical weathering (Schwertmann et al., 2004; Poulton and Raiswell, 2005) also explains our  $\text{Fe}_{\text{ox1}}/\text{Fe}_{\text{T}}$  results. In summary, these results demonstrate that the regulation of  $\text{Fe}_{\text{HR}}/\text{Fe}_{\text{T}}$  ratio by weathering is mainly reflected in the control of  $\text{Fe}_{\text{ox2}}/\text{Fe}_{\text{T}}$  ratio rather than  $\text{Fe}_{\text{ox1}}/\text{Fe}_{\text{T}}$  ratio.

#### 4.2 Relationship between $\text{Fe}_{\text{HR}}$ and TOC

The correlation between  $\text{Fe}_{\text{HR}}$  and TOC was investigated in the sediments of Prydz Bay and the adjacent Southern Ocean. Results show a significant negative correlation between TOC and Al, and TOC and  $\text{Fe}_{\text{T}}$  ( $R^2 = 0.53$ ,  $p < 0.01$ ;  $R^2 = 0.35$ ,  $p < 0.01$ , Figures S2A, B). The source of Fe in the sediments is mainly from weak-weathered rock of the Antarctic continent (see section 4.1), while TOC is mainly derived from primary production by phytoplankton based on organic biomarkers (Zhao et al., 2014) and TOC/TN ratios (Liu et al., 2014). Therefore, the negative correlations indicate significant differences in the sources of TOC (biogenic) versus Al and  $\text{Fe}_{\text{T}}$  (lithogenic), and the dilution relationship between each other.

Previous studies have shown that TOC is often positively correlated with  $\text{Fe}_{\text{HR}}$  in surface sediments from riverine particulates, glaciers and marginal seas (Poulton and Raiswell, 2005; Zhu et al., 2012; Roy et al., 2013; Zhu et al., 2015). However, there is no significant ( $p > 0.05$ ) correlation between the TOC and  $\text{Fe}_{\text{HR}}$ ,  $\text{Fe}_{\text{carb}}$ ,  $\text{Fe}_{\text{ox1}}$  or  $\text{Fe}_{\text{ox2}}$  content in the sediments of our study area (Figures S2C–F), possibly due to the complex sedimentary environment. Based on a wide range of samples, we summarize and classify the relationship between TOC and  $\text{Fe}_{\text{HR}}$  in different sedimentary environments around the world (Figure 6), as follows.

The first scenario pertains to high TOC/ $\text{Fe}_{\text{HR}}$  ratios ( $> 2.5$ ), observed in “Fine” sediments with elevated TOC content ( $1.02\% \pm 0.35\%$ ) and high OC loading ( $\text{TOC}/\text{SSA} = 0.62 \pm 0.33 \text{ mg/m}^2$ ) in this study (Table S3), as well as in anoxic environments like the Black Sea (Wijsman et al., 2001; Jessen et al., 2017). Usually, the extremely high TOC content and TOC/ $\text{Fe}_{\text{HR}}$  ratios in anoxic environments are due to the reduced remineralization of TOC (Jessen et al., 2017). In contrast, “Fine” sediments are mainly located in the center of Prydz Bay, with shallow water depths (251 – 748 m), and high primary productivity ( $412 \text{ mmol C m}^{-2} \text{ d}^{-1}$ ), summer particulate deposition fluxes ( $2515 \pm 1828 \text{ } \mu\text{mol C m}^{-2} \text{ d}^{-1}$ ) and sedimentation rates ( $2.9 - 8.7 \text{ g C m}^{-2} \text{ a}^{-1}$ ) (Behrenfeld and Falkowski, 1997; Yu et al., 2009; Han, 2018). These conditions favor high OC accumulation rates and OC loading (Blair and Aller, 2012). However, the effect of dilution by marine OC on  $\text{Fe}_{\text{HR}}$  content is more significant due to the low  $\text{Fe}_{\text{HR}}$  content caused by inputs of relatively unweathered materials, as described in section 4.1. It should be noted that, unlike in anoxic environments, the situation in our study area is a novel discovery in oxygen-rich polar



marine environments and may have significant global implications for the long-term preservation of marine OC ([Liu et al., 2014](#)).

The second scenario pertains to low TOC/ $Fe_{HR}$  ratios ( $< 0.6$ ), observed in suspended particulates of rivers with high discharge rates (the Amazon River and the Yellow River) ([Poulton and Raiswell, 2005](#)) and deep-sea sediments ([Lalonde et al. \(2012\)](#) and this study). In the former, there are substantial inputs of terrestrial materials (OC and  $Fe_{HR}$ ) to the ocean; however, more than 90% of the OC is remineralized into  $CO_2$  ([Aller and Blair, 2006](#)), and most  $Fe_{HR}$  is oxidized and crystallized into hematite, which has relatively poor bioavailability ([Zhao et al., 2018](#), and references therein), due to frequent physical transformations and rapid redox cycling. In the latter, such as “Ultra-fine” sediments in this study, the prolonged oxygen exposure time of OC in deeper waters ( $> 3000$  m) promotes OC remineralization, and the enhanced weathering leads to more  $Fe_{HR}$  development ([Poulton and Raiswell, 2002](#)).

The third scenario pertains to sediments with both low TOC and  $Fe_{HR}$  content, such as “Coarse” and “Medium” sediments in this study, and in icebergs ([Poulton and Raiswell, 2005](#)). The former are usually located at the front edge of Amery Ice Shelf or in shallow waters where sea ice cover persists for extended periods, resulting in low rates of OC deposition ( $1.1 - 5.7 \text{ g C m}^{-2} \text{ a}^{-1}$ ) ([Yu et al., 2009](#)) and limited TOC accumulation in sediments ([Mayer, 1994](#); [Blair and Aller, 2012](#)). Additionally, weak weathering hinders the development of  $Fe_{HR}$ .

The final scenario pertains to mid-range TOC/ $Fe_{HR}$  ratios (0.6 – 2.5), including typical riverine particulates and marginal shelf sediments ([Poulton and Canfield, 2005](#); [Roy et al., 2013](#)). In this scenario, there is a significant positive correlation between TOC and  $Fe_{HR}$ , as both are derived from terrestrial sources and interact with each other to form OC- $Fe_{HR}$  complexes through adsorption/coprecipitation. These complexes are then transported to the coastal and shelf sediments and preserved for extended periods ([Faust et al., 2021](#)). Therefore, mid-range TOC/ $Fe_{HR}$  ratios represent the characteristics of the residual portion of relatively stable terrestrial OC ([Poulton and Raiswell, 2005](#); [Lalonde et al., 2012](#); [Roy et al., 2013](#); [Faust et al., 2021](#)).

Based on the preceding discussion, we have deduced that the TOC/ $Fe_{HR}$  ratios to some extent can reflect the degree of OC- $Fe_{HR}$  complexing in various environments. This implies that the contribution of  $Fe_{HR}$  to OC preservation may differ across different sedimentary settings. For example, in continental shelf marginal sea sediments with mid-range TOC/ $Fe_{HR}$  ratios, the  $f_{OC-Fe}$  is  $16.1\% \pm 9.5\%$  ( $n = 73$ ) ([Lalonde et al., 2012](#); [Salvadó et al., 2015](#); [Shields et al., 2016](#); [Ma et al., 2018](#); [Faust et al., 2021](#)). In the mobile mud area of the Changjiang Estuary, characterized by low TOC/ $Fe_{HR}$  ratios, the  $f_{OC-Fe}$  is only  $8.1\% \pm 4.2\%$  ( $n = 26$ ) ([Zhao et al., 2018](#)). In the deep-sea sediments with prolonged oxygen exposure, the  $f_{OC-Fe}$  is  $13.7\% \pm 8.7\%$  ( $n = 13$ ) ([Longman et al., 2022](#)). Therefore, we propose that the  $f_{OC-Fe}$  may exhibit significant

variation across different sediment categories in Prydz Bay and the adjacent Southern Ocean. However, research on the  $f_{OC-Fe}$  in Antarctic marine sediments is scarce, with only one Antarctic deep sea sediment out of 406 samples worldwide (Lalonde et al., 2012; Longman et al., 2022). Further research on the  $f_{OC-Fe}$  in Antarctic marine sediments is necessary in consideration of the low  $Fe_{HR}/Fe_T$  ratios and complex TOC/ $Fe_{HR}$  ratios.

## 5 Conclusion

The  $Fe_{HR}/Fe_T$  ratios observed in marine sediments from Prydz Bay and the adjacent Southern Ocean are similar to those in the Antarctic glacial particulates, but lower than those in global riverine particulates and modern marine sediments. This suggests that  $Fe_{HR}$  is mainly derived from the Antarctic bedrock with weak weathering. Our  $Fe_{HR}/Fe_T$  ratios are also lower than those in sediments from the Arctic Barents Sea, off the Antarctic Peninsula and King George Island, likely due to the slower glacier melting. The  $Fe_{ox1}/Fe_T$  ratios in our study area are equivalent to, those in sediments from other continental shelf marginal seas with intense weathering, but the  $Fe_{ox2}/Fe_T$  ratios are lower. This indicates that there is a potential inhibitory effect of low temperatures on aging of iceberg melting  $Fe_{ox1}$ , and the regulation of weathering on  $Fe_{HR}/Fe_T$  ratio is mainly reflected in  $Fe_{ox2}/Fe_T$  ratio. There is no significant correlation between TOC and  $Fe_{HR}$ ,  $Fe_{carb}$ ,  $Fe_{ox1}$  or  $Fe_{ox2}$  content, due to the complex and diverse sedimentary environments in the research region: “Fine” sediments with high TOC/ $Fe_{HR}$  ratios, TOC content, OC loading and low  $Fe_{HR}$  content, “Ultra-fine” sediments with contrary characteristics, and “Medium” and “Coarse” sediments with both low TOC and  $Fe_{HR}$  content.

## Data availability statement

The original contributions presented in the study are included in the article/Supplementary Material. Further inquiries can be directed to the corresponding author.

## Author contributions

WH and JZ made substantial contributions to draft the manuscript. XG and WH made substantial contributions to the data analysis. DL, JH, HZ, CZ, ZH, WS, YS and JP made substantial

contributions to participate the manuscript discussion. All authors contributed to the article and approved the submitted version.

## Funding

This research was jointly supported by the National Natural Science Foundation of China (NSFC) (Nos. 41976228, 42276255, 41976227, 42176227), the Scientific Research Fund of the Second Institute of Oceanography, MNR (No. JG1805), National Polar Special Program “Impact and Response of Antarctic Seas to Climate Change” (Nos. IRASCC 01-01-02A and 02-02), and the China Scholarship Council (No. 201704180017).

## Acknowledgments

The authors would like to thank Dr. Jihao Zhu for helping in  $Fe_T$  determination, and Ms. Huijuan Zhang for grain size measurements. We also extend thanks to the *R/V Xuelong* crews who devoted their time and effort to sample sediments in the CHINARE-24 to -29.

## Conflict of interest

The authors declare that the research was conducted in the absence of any commercial or financial relationships that could be construed as a potential conflict of interest.

## Publisher's note

All claims expressed in this article are solely those of the authors and do not necessarily represent those of their affiliated organizations, or those of the publisher, the editors and the reviewers. Any product that may be evaluated in this article, or claim that may be made by its manufacturer, is not guaranteed or endorsed by the publisher.

## Supplementary material

The Supplementary Material for this article can be found online at: <https://www.frontiersin.org/articles/10.3389/fmars.2023.1142061/full#supplementary-material>

## References

- Aller, R. C., and Blair, N. E. (2006). Carbon remineralization in the Amazon–guianas tropical mobile mudbelt: A sedimentary incinerator. *Cont. Shelf Res.* 26, 2241–2259. doi: 10.1016/j.csr.2006.07.016
- Arrigo, K. R., Van Dijken, G. L., and Strong, A. L. (2015). Environmental controls of marine productivity hot spots around Antarctica. *J. Geophys. Res. Oceans* 120, 5545–5565. doi: 10.1002/2015jc010888
- Behrenfeld, M. J., and Falkowski, P. G. (1997). Photosynthetic rates derived from satellite-based chlorophyll concentration. *Limnol. Oceanogr.* 42, 1–20. doi: 10.2307/2838857
- Bhatia, M. P., Kujawinski, E. B., Das, S. B., Breier, C. F., Henderson, P. B., and Charette, M. A. (2013). Greenland Meltwater as a significant and potentially bioavailable source of iron to the ocean. *Nat. Geosci.* 6, 274–278. doi: 10.1038/ngeo1746

- Blain, S., Queguiner, B., Armand, L., Belviso, S., Bombled, B., Bopp, L., et al. (2007). Effect of natural iron fertilization on carbon sequestration in the southern ocean. *Nature* 446, 1070–1074. doi: 10.1038/nature05700
- Blair, N. E., and Aller, R. C. (2012). The fate of terrestrial organic carbon in the marine environment. *Ann. Rev. Mar. Sci.* 4, 401–423. doi: 10.1146/annurev-marine-120709-142717
- Burdige, D. J., and Christensen, J. P. (2022). Iron biogeochemistry in sediments on the western continental shelf of the Antarctic peninsula. *Geochim. Cosmochim. Acta* 326, 288–312. doi: 10.1016/j.gca.2022.03.013
- Campbell, I. B., Balks, M. R., and Claridge, G. G. C. (1993). A simple visual technique for estimating the impact of fieldwork on the terrestrial environment in ice-free areas of Antarctica. *Polar Res* 29, 321–328. doi: 10.1017/S0032247400023974
- Canfield, D. E. (1989). Reactive iron in marine sediments. *Geochim. Cosmochim. Acta* 53, 619–632. doi: 10.1016/0016-7037(89)90005-7
- Canfield, D. E. (1997). The geochemistry of river particulates from the continental USA: Major elements. *Geochim. Cosmochim. Acta* 61, 3349–3365. doi: 10.1016/S0016-7037(97)00172-5
- Canfield, D. E., Raiswell, R., and Bottrell, S. H. (1992). The reactivity of sedimentary iron minerals toward sulfide. *Amer. J. Sci.* 292, 659–683. doi: 10.2475/ajs.292.9.659
- Dinniman, M. S., St-Laurent, P., Arrigo, K. R., Hofmann, E. E., and Van Dijken, G. L. (2020). Analysis of iron sources in Antarctic continental shelf waters. *J. Geophys. Res. Oceans* 125, 1–19. doi: 10.1029/2019jc015736
- Faust, J. C., Tessin, A., Fisher, B. J., Zindorf, M., Papadaki, S., Hendry, K. R., et al. (2021). Millennial scale persistence of organic carbon bound to iron in Arctic marine sediments. *Nat. Commun.* 12, 275. doi: 10.1038/s41467-020-20550-0
- Folk, R. L. (1980). *Petrology of sedimentary rocks* (Austin Texas: Hemphill Publishing Company), 184pp.
- Han, Z.-B. (2018). “Biological pump” and its response to changes in sea ice in the Prydz Bay, East Antarctic (Wuhan: China University of Geosciences) 135.
- Harris, D., Horwath, W., and Kessel, C. V. (2001). Acid fumigation of soils to remove carbonates prior to total organic carbon or carbon-13 isotopic analysis. *Soil Sci. Soc. Amer. J.* 65, 1853–1856. doi: 10.2136/sssaj2001.1853
- Hawkings, J. R., Wadham, J. L., Tranter, M., Raiswell, R., Benning, L. G., Statham, P. J., et al. (2014). Ice sheets as a significant source of highly reactive nanoparticulate iron to the oceans. *Nat. Commun.* 5, 3929. doi: 10.1038/ncomms4929
- Henkel, S., Kasten, S., Hartmann, J. F., Silva-Busso, A., and Staubwasser, M. (2018). Iron cycling and stable Fe isotope fractionation in Antarctic shelf sediments, King George Island. *Geochim. Cosmochim. Acta* 237, 320–338. doi: 10.1016/j.gca.2018.06.042
- Homoky, W. B., Weber, T., Berelson, W. M., Conway, T. M., Henderson, G. M., Van Hulten, M., et al. (2016). Quantifying trace element and isotope fluxes at the ocean-sediment boundary: A review. *Philos. Trans. A Math. Phys. Eng. Sci.* 374, 1–43. doi: 10.1098/rsta.2016.0246
- Jessen, L. G., Lichtschlag, A., Ramette, A., Pantoja, S., Rossel, E. P., Schubert, C. J., et al. (2017). Hypoxia causes preservation of labile organic matter and changes seafloor microbial community composition (Black Sea). *Sci. Adv.* 3, e1601897. doi: 10.1126/sciadv.1601897
- Katsumata, K., Nakano, H., and Kumamoto, Y. (2015). Dissolved oxygen change and freshening of Antarctic bottom water along 62°S in the Australian-Antarctic basin between 1995/1996 and 2012/2013. *Deep Sea Res. II Top. Stud. Oceanogr.* 114, 27–38. doi: 10.1016/j.dsr2.2014.05.016
- Konhauser, K. O., Kappler, A., and Roden, E. E. (2011). Iron in microbial metabolisms. *Elements* 7, 89–93. doi: 10.1002/chin.201227254
- Kostka, J. E., and Iii, G. (1994). Partitioning and speciation of solid phase iron in saltmarsh sediments. *Geochim. Cosmochim. Acta* 58, 1701–1710. doi: 10.1016/0016-7037(94)90531-2
- Lalonde, K., Mucci, A., Ouellet, A., and Gélinas, Y. (2012). Preservation of organic matter in sediments promoted by iron. *Nature* 483, 198–200. doi: 10.1038/nature10855
- Lin, H., Rauschenberg, S., Hexel, C. R., Shaw, T. J., and Twining, B. S. (2011). Free-drifting icebergs as sources of iron to the Weddell Sea. *Deep Sea Res. II Top. Stud. Oceanogr.* 58, 1392–1406. doi: 10.1016/j.dsr2.2010.11.020
- Liu, R., Yu, P., Hu, C. Y., Han, Z. B., and Pan, J. M. (2014). Contents and distributions of organic carbon and total nitrogen in sediments of Prydz Bay, Antarctica. *Acta Oceanol. Sin.* 36, 118–125. doi: 10.3969/j.issn.0253-4193.2014.04.003
- Longman, J., Faust, J. C., Bryce, C., Homoky, W. B., and März, C. (2022). Organic carbon burial with reactive iron across global environments. *Global Biogeochem. Cycles* 36, e2022GB007447. doi: 10.1029/2022gb007447
- Longman, J., Gernon, T. M., Palmer, M. R., and Manners, H. R. (2021). Tephra deposition and bonding with reactive oxides enhances burial of organic carbon in the Bering Sea. *Global Biogeochem. Cycles* 35, e2021GB007140. doi: 10.1029/2021gb007140
- Lyons, W. B., Dailey, K. R., Welch, K. A., Deuerling, K. M., Welch, S. A., and Mcknight, D. M. (2015). Antarctic Streams as a potential source of iron for the southern ocean. *Geology* 43, 1003–1006. doi: 10.1130/g36989.1
- Ma, W. W., Zhu, M.-X., Yang, G.-P., and Li, T. (2018). Iron geochemistry and organic carbon preservation by iron (oxyhydr)oxides in surface sediments of the East China Sea and the South Yellow Sea. *J. Mar. Syst.* 178, 62–74. doi: 10.1016/j.jmarsys.2017.10.009
- Martin, J. M., and Meybeck, M. (1979). Elemental mass-balance of material carried by major world rivers. *Mar. Chem.* 7, 173–206. doi: 10.1016/0304-4203(79)90039-2
- März, C., Poulton, S. W., Brumsack, H. J., and Wagner, T. (2012). Climate-controlled variability of iron deposition in the central Arctic ocean (southern Mendeleev ridge) over the last 130,000 years. *Chem. Geol.* 330–331, 116–126. doi: 10.1016/j.chemgeo.2012.08.015
- Mathew, D., Gireeshkumar, T. R., Udayakrishnan, P. B., Shameem, K., Nayana, P. M., Deepulal, P. M., et al. (2022). Geochemical speciation of iron under nearshore hypoxia: A case study of alappuzha mud banks, southwest coast of India. *Cont. Shelf Res.* 238, 104686. doi: 10.1016/j.csr.2022.104686
- Mayer, L. M. (1994). Surface area control of organic carbon accumulation in continental shelf sediments. *Geochim. Cosmochim. Acta* 58, 1271–1284. doi: 10.1016/0016-7037(94)90381-6
- Meijers, A. J. S., Klocker, A., Bindoff, N. L., Williams, G. D., and Marsland, S. J. (2010). The circulation and water masses of the Antarctic shelf and continental slope between 30° and 80°E. *Deep Sea Res. II Top. Stud. Oceanogr.* 57, 723–737. doi: 10.1016/j.dsr2.2009.04.019
- Pasquier, V., Fike, D. A., Révillon, S., and Halevy, I. (2022). A global reassessment of the controls on iron speciation in modern sediments and sedimentary rocks: A dominant role for diagenesis. *Geochim. Cosmochim. Acta* 335, 211–230. doi: 10.1016/j.gca.2022.08.037
- Pollard, R. T., Salter, I., Sanders, R. J., Lucas, M. I., Moore, C. M., Mills, R. A., et al. (2009). Southern ocean deep-water carbon export enhanced by natural iron fertilization. *Nature* 457, 577–580. doi: 10.1038/nature07716
- Poulton, S. W., and Canfield, D. E. (2005). Development of a sequential extraction procedure for iron: Implications for iron partitioning in continentally derived particulates. *Chem. Geol.* 214, 209–221. doi: 10.1016/j.chemgeo.2004.09.003
- Poulton, S. W., and Raiswell, R. (2002). The low-temperature geochemical cycle of iron: From continental fluxes to marine sediment deposition. *Amer. J. Sci.* 302, 774–805. doi: 10.2475/ajs.302.9.774
- Poulton, S. W., and Raiswell, R. (2005). Chemical and physical characteristics of iron oxides in riverine and glacial meltwater sediments. *Chem. Geol.* 218, 203–221. doi: 10.1016/j.chemgeo.2005.01.007
- Raiswell, R., and Canfield, D. E. (1998). Sources of iron for pyrite formation in marine sediments. *Amer. J. Sci.* 298, 219–245. doi: 10.2475/ajs.298.3.219
- Raiswell, R., Hawkings, J. R., Benning, L. G., Baker, A. R., Death, R., Albani, S., et al. (2016). Potentially bioavailable iron delivery by iceberg-hosted sediments and atmospheric dust to the polar oceans. *Biogeochemistry* 13. doi: 10.3389/feart.2018.00222
- Raiswell, R., Hawkings, J., Elsenousy, A., Death, R., Tranter, M., and Wadham, J. (2018). Iron in glacial systems: Speciation, reactivity, freezing behavior, and alteration during transport. *Front. Earth Sci.* 6. doi: 10.3389/feart.2018.00222
- Raiswell, R., Tranter, M., Benning, L. G., Siegert, M., De'ath, R., Huybrechts, P., et al. (2006). Contributions from glacially derived sediment to the global iron (oxyhydr) oxide cycle: Implications for iron delivery to the oceans. *Geochim. Cosmochim. Acta* 70, 2765–2780. doi: 10.1016/j.gca.2005.12.027
- Roy, M., Mcmanus, J., Goñi, M. A., Chase, Z., Borgeld, J. C., Wheatcroft, R. A., et al. (2013). Reactive iron and manganese distributions in seabed sediments near small mountainous rivers off Oregon and California (USA). *Cont. Shelf Res.* 54, 67–79. doi: 10.1016/j.csr.2012.12.012
- Rueckamp, M., Braun, M., Suckro, S., and Blindow, N. (2011). Observed glacial changes on the King George Island ice cap, Antarctica, in the last decade. *Global Planet. Change* 79, 99–109. doi: 10.1016/j.gloplacha.2011.06.009
- Salvadó, J. A., Tesi, T., Andersson, A., Ingrid, J., Dudarev, O. V., Semiletov, I. P., et al. (2015). Organic carbon remobilized from thawing permafrost is resequenced by reactive iron on the Eurasian Arctic shelf. *Geophys. Res. Lett.* 42, 8122–8130. doi: 10.1002/2015gl066058
- Schwertmann, U., Stanjek, H., and Becher, H. H. (2004). Long-term *in vitro* transformation of 2-line ferrihydrite to goethite/hematite at 4, 10, 15 and 25°C. *Clay Miner.* 39, 433–438. doi: 10.1180/0009855043940145
- Screen, J. A., and Simmonds, I. (2010). Increasing fall-winter energy loss from the Arctic ocean and its role in Arctic temperature amplification. *Geophys. Res. Lett.* 37, L16707. doi: 10.1029/2010gl044136
- Senn, A.-C., Kaegi, R., Hug, S. J., Hering, J. G., Mangold, S., and Voegelin, A. (2017). Effect of aging on the structure and phosphate retention of Fe(III)-precipitates formed by Fe(II) oxidation in water. *Geochim. Cosmochim. Acta* 202, 341–360. doi: 10.1016/j.gca.2016.12.033
- Shepherd, A., Fricker, H. A., and Farrell, S. L. (2018). Trends and connections across the Antarctic cryosphere. *Nature* 558, 223–232. doi: 10.1038/s41586-018-0171-6
- Shields, M. R., Bianchi, T. S., Gélinas, Y., Allison, M. A., and Twilley, R. R. (2016). Enhanced terrestrial carbon preservation promoted by reactive iron in deltaic sediments. *Geophys. Res. Lett.* 43, 1149–1157. doi: 10.1002/2015gl067388
- Stammerjohn, S. E., Martinson, D. G., Smith, R. C., and Iannuzzi, R. A. (2008). Sea Ice in the western Antarctic peninsula region: Spatio-temporal variability from ecological and climate change perspectives. *Deep Sea Res. II Top. Stud. Oceanogr.* 55, 2041–2058. doi: 10.1016/j.dsr2.2008.04.026
- Tagliabue, A., Bowie, A. R., Boyd, P. W., Buck, K. N., Johnson, K. S., and Saito, M. A. (2017). The integral role of iron in ocean biogeochemistry. *Nature* 543, 51–59. doi: 10.1038/nature21058
- Taylor, S. R. (1964). Abundance of chemical elements in the continental crust: A new table. *Geochim. Cosmochim. Acta* 28, 1273–1285. doi: 10.1016/0016-7037(64)90129-2
- Thamdrup, B. (2000). Bacterial manganese and iron reduction in aquatic sediments. *Adv. Microbial Ecol.* 16, 41–84. doi: 10.1007/978-1-4615-4187-5\_2
- The IMBIE team (2018). Mass balance of the Antarctic ice sheet from 1992 to 2017. *Nature* 558, 219–222. doi: 10.1038/s41586-018-0179-y

- Thomasarrigo, L. K., Kaegi, R., and Kretzschmar, R. (2019). Ferrihydrite growth and transformation in the presence of ferrous iron and model organic ligands. *Environ. Sci. Technol.* 53, 13636–13647. doi: 10.1021/acs.est.9b03952
- Vaz, R., and Lennon, G. W. (1996). Physical oceanography of the prydzh bay region of Antarctic waters. *Deep Sea Res. I Oceanogr. Res. Pap.* 43, 603–641. doi: 10.1016/0967-0637(96)00028-3
- Wadley, M. R., Jickells, T. D., and Heywood, K. J. (2014). The role of iron sources and transport for southern ocean productivity. *Deep Sea Res. I Oceanogr. Res. Pap.* 87, 82–94. doi: 10.1016/j.dsr.2014.02.003
- Wang, D., Zhu, M. X., Yang, G. P., and Ma, W. W. (2019). Reactive iron and iron-bound organic carbon in surface sediments of the river-dominated bohai Sea (China) versus the southern yellow Sea. *J. Geophys. Res. Biogeosci.* 124, 79–98. doi: 10.1029/2018jg004722
- Wehrmann, L. M., Formolo, M. J., Owens, J. D., Raiswell, R., Ferdelman, T. G., Riedinger, N., et al. (2014). Iron and manganese speciation and cycling in glacially influenced high-latitude fjord sediments (West spitsbergen, svalbard): Evidence for a benthic recycling-transport mechanism. *Geochim. Cosmochim. Acta* 141, 628–655. doi: 10.1016/j.gca.2014.06.007
- Wei, G.-Y., Chen, T., Poulton, S. W., Lin, Y.-B., He, T., Shi, X., et al. (2021). A chemical weathering control on the delivery of particulate iron to the continental shelf. *Geochim. Cosmochim. Acta* 308, 204–216. doi: 10.1016/j.gca.2021.05.058
- Wijsman, J. W. M., Middelburg, J. J., and Heip, C. H. R. (2001). Reactive iron in black Sea sediments: Implications for iron cycling. *Mar. Geol.* 172, 167–180. doi: 10.1016/S0025-3227(00)00122-5
- Williams, G. D., Herraiz-Borreguero, L., Roquet, F., Tamura, T., Ohshima, K. I., Fukamachi, Y., et al. (2016). The suppression of Antarctic bottom water formation by melting ice shelves in prydzh bay. *Nat. Commun.* 7, 12577. doi: 10.1038/ncomms12577
- Wu, L., Wang, R., Xiao, W., Ge, S., Chen, Z., and Krijgsman, W. (2017). Productivity-climate coupling recorded in pleistocene sediments off prydzh bay (East Antarctica). *Palaeogeogr. Palaeoclimatol. Palaeoecol.* 485, 260–270. doi: 10.1016/j.palaeo.2017.06.018
- Yu, P., Hu, C., Liu, X., Pan, J., and Zhang, H. (2009). Modern sedimentation rates in Prydz Bay, Antarctic. *Acta Sedimentol. Sin.* 27, 1172–1177.
- Zhao, J., Peter, H.-U., Zhang, H., Han, Z., Hu, C., Yu, P., et al. (2014). Short- and long-term response of phytoplankton to ENSO in prydzh bay, Antarctica: Evidences from field measurements, remote sensing data and stratigraphic biomarker records. *J. Ocean Univ. China* 13, 437–444. doi: 10.1007/s11802-014-2231-3
- Zhao, B., Yao, P., Bianchi, T. S., Shields, M. R., Cui, X. Q., Zhang, X. W., et al. (2018). The role of reactive iron in the preservation of terrestrial organic carbon in estuarine sediments. *J. Geophys. Res. Biogeosci.* 123, 3556–3569. doi: 10.1029/2018jg004649
- Zhu, M.-X., Hao, X.-C., Shi, X.-N., Yang, G.-P., and Li, T. (2012). Speciation and spatial distribution of solid-phase iron in surface sediments of the East China Sea continental shelf. *Appl. Geochem.* 27, 892–905. doi: 10.1016/j.apgeochem.2012.01.004
- Zhu, M.-X., Huang, X.-L., Yang, G.-P., and Chen, L.-J. (2015). Iron geochemistry in surface sediments of a temperate semi-enclosed bay, north China. *Estuar. Coast. Shelf Sci.* 165, 25–35. doi: 10.1016/j.ecss.2015.08.018